J Mol Model (2005) 11: 97–104
DOI 10.1007/s00894-004-0225-6

ORIGINAL PAPER

Qing-Chuan Zheng · Ze-Sheng Li · Jing-Fa Xiao
Miao Sun · Yuan Zhang · Chia-Chung Sun

Homology modeling and PAPS ligand (cofactor) binding study of bovine phenol sulfotransferase

Received: 5 June 2004 / Accepted: 3 November 2004 / Published online: 15 March 2005

Abstract In order to understand the mechanisms of ligand binding and the interaction between the ligand and the bovine phenol sulfotransferase, (bSULT1A1, EC 2.8.2.1) a three-dimensional (3D) model of the bSULT1A1 is generated based on the crystal structure of the estrogen sulfotransferase (PDB code 1AQU) by using the InsightII/Homology module. With the aid of the molecular mechanics and molecular dynamics methods, the final refined model is obtained and is further assessed by Profile-3D and ProStat, which show that the refined model is reliable. With this model, a flexible docking study is performed and the results indicate that 3′-phosphoadenosine-5′- phosphosulfate (PAPS) is a more preferred ligand than coenzyme A (CoA), and that His108 forms hydrogen bond with PAPS, which is in good agreement with the experimental results. From these docking studies, we also suggest that Phe255, Phe24 and Tyr169 in bSULT1A1 are three important determinant residues in binding as they have strong van-der-Waals contacts with the ligand. The hydrogen–bonding interactions also play an important role for the stability of the complex. Our results may be helpful for further experimental investigations.

Keywords Bovine phenol sulfotransferase · Docking · Molecular dynamics

Introduction

Sulfate conjugation is an important pathway in the biotransformation of many drugs, xenobiotics, neurotransmitters, steroids, and other hormones [1–4]. Sulfate conjugation is mainly catalyzed by cytosolic sulfotransferase enzymes. The sulfotransferase enzymes can alter biological activities of numerous carcinogenic and mutagenic compounds and play an important role in chemical defense mechanisms through sulfation [5]. bSULT1A1 belongs to a family of cytosolic sulfotransferase enzymes [6]. The sulfotransferase uses 3′-phosphoadenosine-5′-phosphosulfate (PAPS) as a donor of the sulfonate (sulfuryl) group and transfers the sulfonate group from PAPS to an acceptor substrate to form either a sulfate ester or a sulfamate [7].

In 1999, Leach et al. [8] reported that for the bSULT1A1, CoA is a competitive inhibitor with respect to the sulfuryl donor substrate, PAPS. Recently, the structure of human SULT1A1 (PDB code 1LS6) crystallized in the presence of 3′-phosphoadenosine-5′-phosphate (PAP) and *p*-nitrophenol (*p*NP) was reported by Gamage et al. [9] and this structure suggested an extended and very hydrophobic binding site. Gamage's work gives the first sulfotransferase structure complexed with a xenobiotic substrate. However, up to now no report has been found about the three-dimensional (3D) structure of the bSULT1A1, and thus theoretical studies on the binding mode of the bSULT1A1 with its inhibitors are necessary to reveal the interaction occurring in the active site.

The phenol sulfotransferase family can be subdivided further into at least two "subfamilies," i.e. the phenol sulfotransferases and the estrogen sulfotransferases [6, 10, 11]. In this paper, we try to obtain a reliable 3D structure of bSULT1A1 based on estrogen sulfotransferase (EC 2.8.2.4, PDB code 1AQU) [12] by the InsightII/Homology method and molecular mechanics and molecular dynamics simulations. The model structure is then used to search the active site and carry out binding studies by flexible docking with the PAPS ligand (cofactor).

The docked complex would be used to identify the key residues for revealing further the ligand reaction mechanism, in particular identifying the binding residues

Q.-C. Zheng · Z.-S. Li (✉) · J.-F. Xiao · M. Sun · Y. Zhang
C.-C. Sun
State Key Laboratory of Theoretical and Computational Chemistry, Institute of Theoretical Chemistry,
Jilin University, Changchun, 130023,
Peopie's Republic of China
E-mail: zeshengli@mail.jlu.edu.cn
Tel.: +86-431-8498960
Fax: +86-431-8498026

with the candidates PAPS and CoA and identifying the more preferred ligand.

Theory and methods

All simulations are performed on SGI O3800 workstations using the InsightII software package developed by Biosym Technologies [13]. The sequence of bSULT1A1 was obtained from the databank in the National Center for Biotechnology Information (http://www.ncbi.nlm.nih.gov). The consistent-valence forcefield (CVFF) was used for energy minimization (EM) and molecular dynamics (MD) simulations.

3D model building

The homology module [14] was used to build the initial model of bSULT1A1.

The first step is searching a number of related sequences to find a related protein as a template by the FASTA program [15–17]. The high sequence identity between bSULT1A1 and the reference protein 1AQU is 49.6%, which allowed for rather straightforward sequence alignment (see Fig. 1). In the second step, the backbone coordinates of the residues in bSULT1A1 were generated with the InsightII/Homology module. The structurally conserved regions (SCRs) were determined by multiple sequence alignment, which is based on the Needleman and Wunsch Algorithm [18], and the coordinates of SCRs in bSULT1A1 were generated by copying from 1AQU.

Variable regions (VRs) are defined as the sections of the proteins that exist between the SCRs in the sequence [14]. To construct the structural variable regions, a loop-searching algorithm over the databank of known crystal structure was used [19]. The residues at the N-termini and C-termini were generated with the END-repair method provided by the InsightII/Homology program. For the remaining side chains, library values of rotamers were adopted. Through the procedure mentioned above, an initial model was thus generated.

The initial model was improved by EM. After 200 steps of conjugate gradient (CG) minimization performed, an MD simulation was carried out to examine the quality of the model structures by checking their stability via performing 150 ps simulations at a constant temperature of 298 K. An explicit solvent model TIP3P water was used. The homology solvent model was constructed with a 10 Å water cap from the center of mass of bSULT1A1. Finally, a conjugate gradient energy minimization of the full protein was performed until the root mean-square (rms) gradient was lower than 0.001 kcal mol^{-1}, $Å^{-1}$. All calculations mentioned above used the Discover3 software package [20]. In this step, the quality of the initial model was improved.

After the optimization procedure, the structure was checked by Profile-3D [21, 22] and ProStat. The Profile-3D method measures the compatibility of an amino-acid sequence with a known 3D protein structure. This is especially useful in the final phase of the protein structure modeling. The ProStat module of InsightII identifies and lists the number of instances where structural features differ significantly from the average values calculated from known proteins.

Binding-site analysis

The Binding-site module [23] is a suite of programs in InsightII for identifying and characterizing protein active sites, binding sites, and functional residues from protein structures and multiple sequence alignments. In this study, ActiveSite-Search was used to identify protein active sites and binding sites by locating cavities in

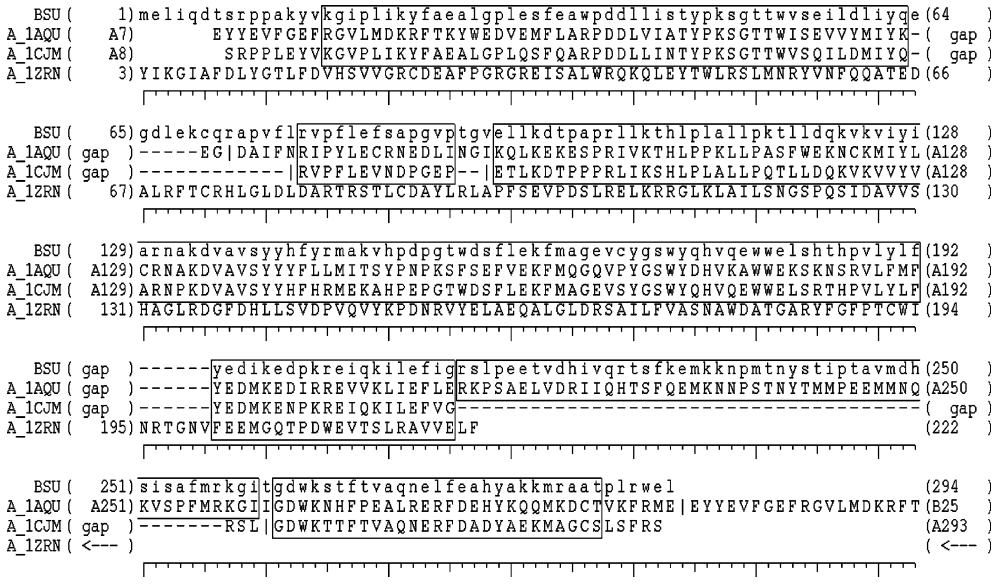

Fig. 1 Multiple sequence alignment of bSULT1A1 with aryl sulfotransferase (PDB code: 1CJM), estrogen sulfotransferase (PDB code: 1AQU) and L-2-haloacid dehalogenase (PDB code: 1ZRN). The SCRs are label with **boxes**

the bSULT1A1 structure. When the search is complete, the largest site is automatically displayed on the structure. Then, by using Asite-Display, two other sites were also obtained. The results can be used to guide the protein-ligand docking experiment.

Docking ligands to bSULT1A1

Affinity, which uses a combination of Monte Carlo type and Simulated Annealing procedures to dock, is a suite of programs for automatically docking a ligand (guest) to a receptor (host) [24]. By means of the 3D structure of PAPS and CoA, which were built through the InsightII/Builder program, the automated molecular docking was performed by using the docking program affinity. A key feature is that the "bulk" of the receptor, defined as atoms that are not in the binding (active) site specified, is held rigid during the docking process, while the binding site atoms and ligand atoms are movable. The potential function of the complex was assigned using the CVFF and the cell-multipole approach was used for non-bonding interactions. To account the solvent effect, the centered enzyme-ligand complexes were solvated in a sphere of TIP3P water molecules with radius 10 Å. Finally, the docked complex of bSULT1A1 with PAPS or with CoA was selected by the criterion of interacting energy combined with the geometrical matching quality. These complexes were used as the starting conformation for further energetic minimization and geometrical optimization before the final models were generated.

Result and discussion

Homology modeling of bSULT1A1

A high level of sequence identity should guarantee more accurate alignment between the target sequence and template structure. In the result of the FASTA search, only three reference proteins, including aryl sulfotransferase (PDB code 1CJM) [25], estrogen sulfotransferase (PDB code 1AQU) and L-2-haloacid dehalogenase (EC 3.8.1.2, PDB code 1ZRN) [26], have a high level of sequence identity and the sequence identities of these three reference proteins identity with bSULT1A1 are 78.9, 49.6, and 34.9%, respectively. In order to define SCRs of the protein family, multiple sequence alignment based on the structural conservative was used to superimpose the three reference structures, and the SCRs were determined as shown by Fig. 1. Then, the Needleman–Wunsch algorithm with the identity matrix was used to align the amino-acid sequence of bSULT1A1 to the SCRs. Because of the long variable regions alignment, it is difficult to assign coordinates based on 1CJM. From Fig. 1 we know that 1ZRN is not more closely related to the sulfotransferase structure. In the following study, we reject 1CJM and 1ZRN and choose 1AQU as the reference for modeling the target protein. After assigning coordinates from the reference protein (1AQU) to the SCRs, we further assign coordinates from the reference loop region to VRs, and coordinates of N-termini and C-termini. All the side chains of the model protein were set by rotamers. With this procedure, the initial model was generated.

After the initial model was complete, we searched the possible active sites using the Binding-Site module and compared these results with the active site of 1AQU [12]. Thus, we know that residues 1–15 and 289–294 do not locate near the active site. In our study, residues 1–15 and 289–294 of bSULT1A1 are removed from the model because no homologous region occurrs in 1AQU and these residues do not locate near the active site. Thus, the model is made up of residues 16–288. This model was refined by MM optimization and MD simulations, and the final stable structure of bSULT1A1 was obtained, as shown in Fig. 2. From Fig. 2 we can see that this enzyme has nine helices and three sheets. An analysis by ProStat shows that there is no significant difference between the calculated values of the bond lengths and bond angles and that of the known proteins for the total residues. The final structure was further checked by profile-3D and the results are shown in Fig. 3. Note that compatibility scores above zero correspond to 'acceptable' side chain environments. From Fig. 3, we can see that all residues are reasonable, which make us to believe that the structure of bSULT1A1 is reliable. It should be pointed out that the crystal structure of 1LS6 was solved during our study [9]. However, it was published too late for us to use it as a starting model in our study. Despite this, 1LS6 can be employed to testify the rationality of the final model. Figure 4 shows the structure alignment of Cα trace between bSULT1A1 and 1LS6. The root mean square deviation of the Cα atoms (Cα RMSD) between bSULT1A1 and 1LS6 is 0.81 Å, which further indicates that the homology model is reliable.

Fig. 2 The final 3D-structure of bSULT1A1. The structure is obtained by energy minimizing an average conformation over the last 100 ps of MD simulation. The α-helix is represented in *red* and the β-sheet in *yellow*

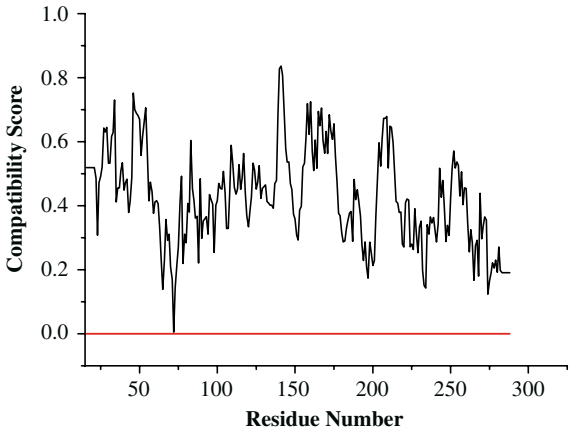

Fig. 3 The 3D profiles verified results of bSULT1A1 model, residues with positive compatibility score are reasonably folded

Identification of PAPS ligand (cofactor)-binding region in bSULT1A1

Three active sites are obtained using InsightII/Binding-Site module, and the locations of the three sites in the 3D structures of bSULT1A1 are shown in Fig. 5. bSULT1A1 and 1AQU are well conserved in both sequence and structure, their biological functions should be identical. Thus, we suggest that PAPS binds in a similar manner for both 1AQU and bSULT1A1. In fact, from the sequence alignment of bSULT1A1 with 1AQU, we know that the residues Lys48, Ser49, Gly50, Thr51, Thr52, Trp53, Lys106, His108, Arg130, Ser138, Phe142, Tyr193, Thr227, Ser228, Phe229, Met232, Phe255, Met256, Arg257, Lys258 and Gly259 are conserved. By considering the experimental fact that the active site of 1AQU includes all the residues mentioned above, and on the other hand, among the three sites, the shape of site 1 (red region) in bSULT1A1 is similar to that of the catalytic site in mouse estrogen sulfotransferase, which has been observed by Kakuta et al. [12] and the 1AQU PAP binding site contains site 1. Thus, in this study site 1 is chosen as the more favorable binding site to dock the ligand, and the other two sites are not discussed further.

Docking study

All reports suggest that PAPS can bind to the enzyme in the absence of a phenol. We are interested in testing the roles of the charged phosphate and sulfate groups of PAPS in binding to bSULT1A1. CoA, one of the endogenous inhibitors, fulfills several metabolic and regulatory roles, and is of interest because of its overt structural overlap with PAPS. Leach et al. [8] and Tulik et al. [27] have demonstrated the inhibition of bSULT1A1 by CoA. In the following discussion, the interactions of the ligands with the receptor in the modeled complexes are investigated, and we shall compare the inhibition ability of bSULT1A1 by PAPS with that by CoA.

The molecular structure of PAPS and CoA were built and optimized by the InsightII/Builder program. The final structure is shown in Fig. 6.

Docking of the ligand into the active site

To understand the interaction between bSULT1A1 and PAPS, the PAPS– bSULT1A1 (P–b) complex was generated using the InsightII/Affinity module and the binding 3D conformation of the P–b complex is shown

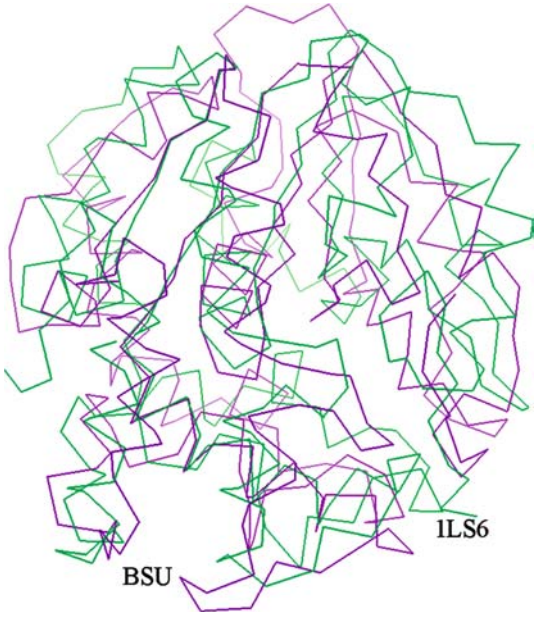

Fig. 4 Cα trace of bSULT1A1 (represented by *purple color*) and 1LS6 (represented by *green color*)

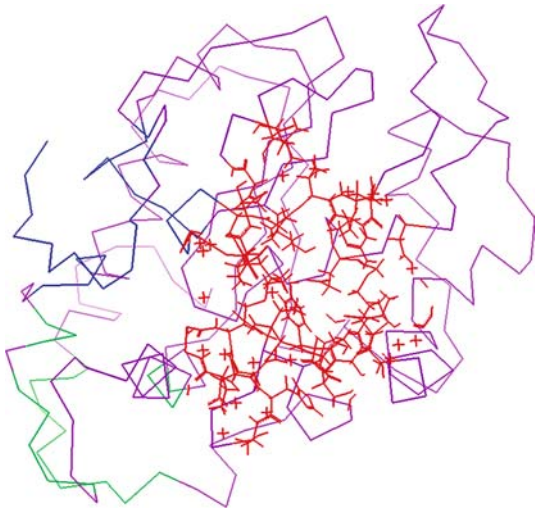

Fig. 5 The possible binding-site of bSULT1A1 model. Site 1 represented by *red color*. Site 2 represented by *green color*. Site 3 represented by *blue color*

in Fig. 7. This figure shows that PAPS locates in the center of the active site, and is stabilized by hydrogen bonding and hydrophobic interactions. Hydrogen bonds play an important role for structure and function of biological molecules, especially for enzyme catalysis. The hydrogen bonds present in the P–b complex are listed in Table 1 and Fig. 8. There are two hydrogen bonds between the carbonyl O of Glu56 and phosphate H of PAPS. The ribose hydroxyl group of PAPS is tightly bound to the amino H of His108 by a hydrogen bond. The amino H of Lys106 forms two hydrogen bonds with the sulfate and phosphate O's of PAPS. It should be pointed out that, with the aid of H_2O, two pairs of hydrogen bonds are also formed between bSULT1A1 and PAPS. One is formed between the carbonyl O of Arg78 and the sulfate H of PAPS by taking H_2O as a bridge. Another one is formed between the side-chain S of Met145 and the phosphate H of PAPS via H_2O. These hydrogen bonding interactions enhance the stability of the P–b complex. Among these hydrogen–bonding interactions, we think that Lys106 and Glu56 are the main contributors to the P–b complex because Lys106 and Glu56 form two hydrogen bonds with PAPS.

To determine the key residues that comprise the active site of the model, the interaction energies of the ligand with each of the residues in the active site of bSULT1A1 were calculated. Significant binding-site residues in the models are identified by the total interaction energy between the ligand and each amino acid residues in the enzyme. This identification, compared with a definition based on the distance from the ligand, can clearly show the relative significance for every residue. Table 2 gives the interaction energies including the total, van-der-Waals and electrostatic energies with the total energies lower than -1.00 kcal mol^{-1} for all residues in the P–b complex. From Table 2 we can also see that the P–b complex has a large favorable total interaction energy of -71.70 kcal mol^{-1}, the van-der-Waals and electrostatic energies are -51.94 and -19.76 kcal mol^{-1}, respectively. These results indicate that both the van-der-Waals and electrostatic energies are important for the P–b complex interaction. Through interaction analysis, we know that Glu56, His108, Tyr240, Phe255, Phe24, Pro80, Phe142, Tyr169, and Pro47 are important anchoring residues for PAPS and are the main contributors to the ligand interaction. Lys106 is not listed in Table 2 as having a total calculated bonding energy more than -1 kcal mol^{-1}. We think that Lys106 may be an important residue because it forms a hydrogen bond with PAPS. It should be noted that His108, Phe255, and Phe142 are important anchoring residues, as proposed by Kakuta et al. [12] and this conclusion is identical with our result. From the alignment result, we can see that these nine residues are highly conserved in the three enzymes. For the hydrophobic residues of Tyr240, Phe255, Phe24, Pro80, Phe142, Tyr169, and Pro47, the interaction energies with PAPS consist mainly of van-der-Waals interactions. The total interaction energy between PAPS and Glu56 is -23.73 kcal mol^{-1} in which the primary interaction energy is electrostatic (E_{ele} = -23.83 kcal mol^{-1}).

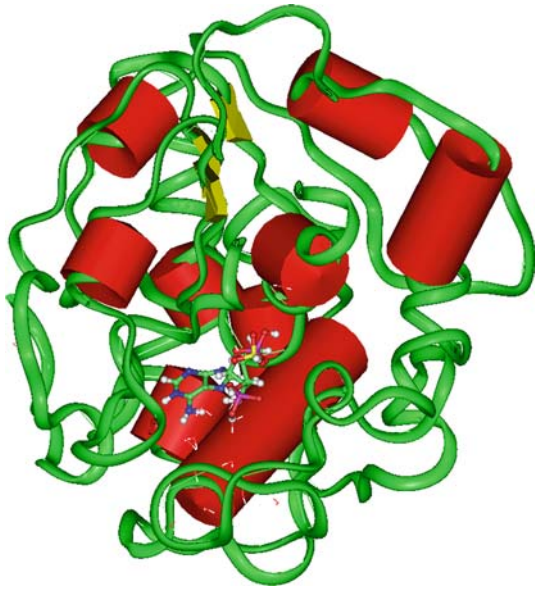

Fig. 7 A stereo picture of the 3D-structure of complex bSULT1A1–PAPS

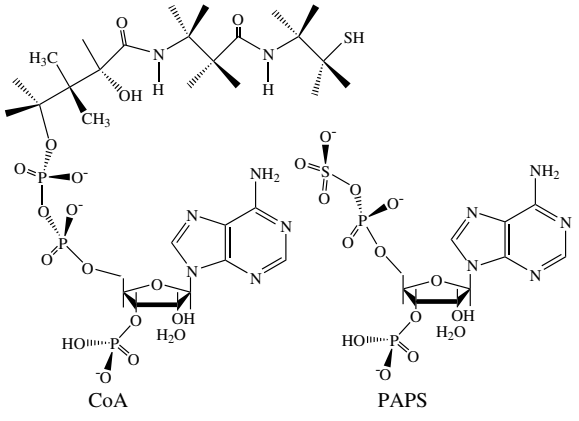

Fig. 6 The structures of PAPS and coenzyme A

Table 1 The hydrogen bonds between ligand (PAPS or CoA) and active site residues of bSULT1A1

bSULT1A1		PAPS atom	CoA atom	Distance (Å)	Angle (°)
Residue	Atom				
Glu56	O	Phosphate H		1.64	161.64
Glu56	O	Phosphate H		2.13	130.43
Lys 106	H	Sulfate O		1.82	140.63
Lys 106	H	Phosphate O		2.22	132.35
His 108	H	Ribose O		2.21	143.89
Tyr 139	O		Phosphate H	1.90	145.31
Phe 142	O		Phosphate H	1.97	158.22
Met 145	S		Adenine N	2.68	NA

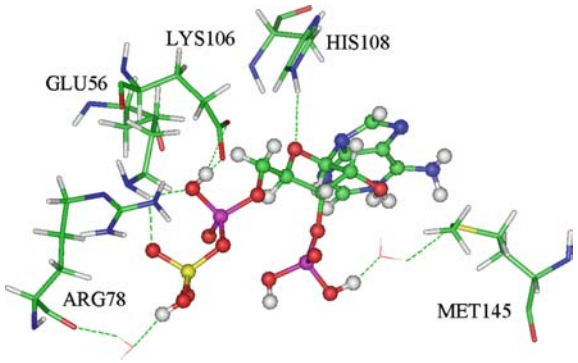

Fig. 8 The hydrogen bonding interaction of complex bSULT1A1–PAPS

Docking of the inhibitor into the active site

To understand the interaction between bSULT1A1 and CoA, the CoA- bSULT1A1(C–b) complex was generated using the InsightII/Affinity module. The binding 3D conformation of the C–b complex is shown in Fig. 9. CoA also locates in the center of the active site, and there are three hydrogen bonds between bSULT1A1 and CoA. However, there is no hydrogen bond between bSULT1A1 and CoA that uses H_2O as a bridge (Table1 and Fig. 10). The Phosphate H of CoA forms two hydrogen bonds with the carbonyl O of Tyr139 and Phe142. The adenine ring of CoA is tightly bound by one hydrogen bond with the side-chain S of Met145.

To determine the key residues that comprise the active site of the model, the interaction energies of the inhibitor with each residue in the active site of bSULT1A1 were calculated. Table 3 gives these interaction energies including the total, van-der-Waals and electrostatic energies, for all residues with a total energy lower than -1.00 kcal mol^{-1} in the C–b complex. From Table 3 we can see that the C–b complex has a large favorable total interaction energy of -75.55 kcal mol^{-1}, the van-der-Waals and electrostatic energies are -59.61 and -15.94 kcal mol^{-1}, respectively. From this result, we suggest that Tyr139, Tyr143, Phe142, Phe84, Phe81, Phe24, Tyr169, Glu83, phe255, Met248, His108, and Cys168 are important anchoring residues for CoA and are the main contributors to the inhibitor interaction. Met145 is not listed in Table 3 as having a total calculated bonding energy more than -1 kcal mol^{-1}. However, we think that Met145 may be an important residue because it forms a hydrogen bond with CoA. From the alignment result, we can see that these 12 residues, except for Tyr143, Phe84, and Cysh168 are highly conserved in the three enzymes, and that the nine highly conserved residues in bSULT1A1 are important for enzyme catalysis. For the hydrophobic residues

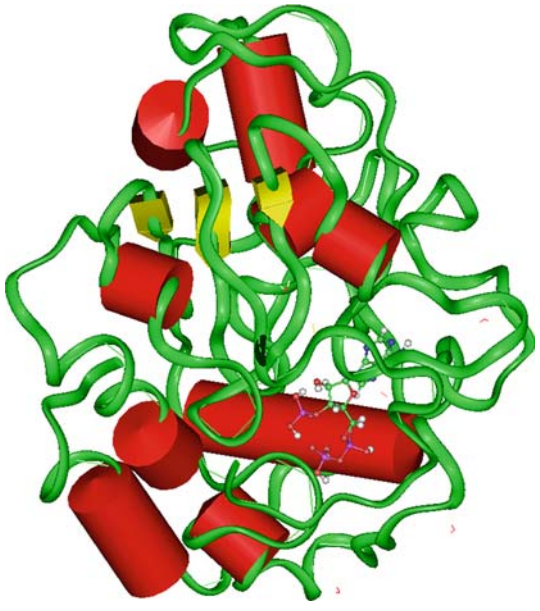

Fig. 9 A stereo picture of the 3D-structure of complex bSULT1A1–CoA

Table 2 The total energy (E_{total}), van-der-Waals energy (E_{vdw}) and electrostatic energy (E_{ele}) between PAPS and individual residues ($E_{total} < -1.00$ kcal mol^{-1} listed in energy rank order)

Residue	E_{vdw} (kcal mol^{-1})	E_{ele} (kcal mol^{-1})	E_{total} (kcal mol^{-1})
Total	−51.94	−19.76	−71.70
Glu 56	0.10	−23.83	−23.73
His 108	−5.78	−1.94	−7.72
Tyr 240	−3.48	−1.58	−5.06
Phe 255	−5.54	0.78	−4.76
Phe 24	−3.01	−1.05	−4.06
Pro 80	−2.40	−1.00	−3.40
Phe 142	−3.14	−0.09	−3.23
Tyr 169	−2.06	−0.50	−2.56
Pro 47	−2.14	−0.31	−2.45
Met 248	−1.89	0.10	−1.79
Arg 78	−4.06	2.33	−1.73
Met 145	−1.72	0.09	−1.63
Asp 249	−0.37	−0.80	−1.17
Thr 51	−0.61	−0.55	−1.16
Thr 107	−0.61	−0.46	−1.07
Phe 84	−1.41	0.41	−1.0
Met 237	−1.44	0.44	−1.0

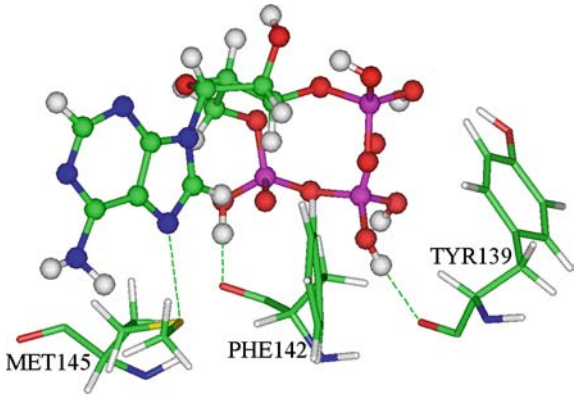

Fig. 10 The hydrogen bonding interaction of complex bSULT1A1–CoA

Table 3 The total energy (E_{total}), van-der-Waals energy (E_{vdw}) and electrostatic energy (E_{ele}) between CoA and individual residues ($E_{total} < -1.00$ kcal mol^{-1} listed in energy rank order)

Residue	E_{vdw} (kcal mol^{-1})	E_{ele} (kcal mol^{-1})	E_{total} (kcal mol^{-1})
Total	−59.61	−15.94	−75.55
Tyr 139	−5.98	−6.32	−12.3
Tyr 143	−5.08	−2.74	−7.82
Phe 142	−2.27	−4.47	−6.74
Phe 84	−6.20	0.62	−5.58
Phe 81	−5.31	0.26	−5.05
Phe 24	−3.29	−0.67	−3.96
Tyr 169	−2.56	−1.07	−3.63
Glu 83	−3.25	−0.36	−3.61
Phe 255	−3.54	0.10	−3.44
Met 248	−2.75	−0.22	−2.97
His 108	−3.70	1.01	−2.69
Cysh 168	−1.79	−0.74	−2.53
Tyr 46	−2.14	−0.17	−2.31
His 149	−2.40	0.56	−1.84
Asp 249	−1.12	−0.59	−1.71
Tyr 140	−0.50	−1.08	−1.58
His 141	−0.62	−0.78	−1.40
Val 247	−1.98	0.65	−1.33
Ser 138	−0.46	−0.63	−1.09

Phe84, Phe81, Phe24, Tyr169, Phe255, Met248, and Cys168, the interaction energies with CoA consist mainly of van-der-Waals interactions. Especially, the van-der-Waals and electrostatic energies between the Tyr139 and CoA are −5.98 and −6.32 kcal mol^{-1}, between the Phe142 and CoA are −2.27 and −4.47 kcal mol^{-1}, respectively. We can conjecture that the primary interaction energy is electronic interaction one as the Tyr139 and Phe142 form hydrogen bond with CoA.

In summary, the above results show that the total interaction energy between bSULT1A1 and PAPS is higher than that between bSULT1A1 and CoA. The number of hydrogen bonds in the P–b complex is more than that in the C–b complex. This means that the P–b complex is more stable than that of the C–b complex. Furthermore, there are many common important residues in the bSULT1A1 binding to CoA and PAPS. This indicates that there is a simple competitive inhibition between PAPS and CoA, and PAPS is the more preferred ligand. This result is consistent with the experimental facts [8]. In our studies, His108 is important for a strong hydrogen-bonding interaction with PAPS, which is in good agreement with the experiment by Gamage et al. [9]. On the other hand, the residues Phe255, Phe24, and Tyr169 in bSULT1A1 are three important determinants in binding as they have strong van-der-Waals contacts with the ligand. As shown in Tables 2 and 3, these results can serve as a guide for the selection of candidate sites for further experimental studies of site-directed mutagenesis.

Conclusions

In this work, we have constructed a 3-D model of bSULT1A1 using the InsightII/Homology module. After energy minimization and molecular dynamics simulations, this refined model structure is obtained. The final refined model was assessed further by Profile-3D and ProStat, and the results show that this model is reliable. The stable structure is further used for docking of PAPS and CoA. Through the docking studies, the model structures of the ligand-receptor complex were obtained. The docking results indicate that conserved amino-acid residues in bSULT1A1 play an important role in maintaining a functional conformation and are directly involved in donor substrate binding. The interactions of bSULT1A1 and PAPS or CoA proposed in this study are useful for understanding the potential mechanisms of bSULT1A1 and the ligand. In particular, with the aid of H_2O some hydrogen bonds are formed in the docked complex. As is well known, hydrogen bonds play an important role for the structure and function of biological molecules, especially for enzyme catalysis. His108 is important for strong hydrogen-bonding interaction with PAPS, which is in good agreement with the experiment by Gamage et al. [9]. It is noticeable that PAPS is a more preferred ligand and that there is a simple competitive inhibition between PAPS and CoA, which is consistent with the experimental facts [8, 27]. On the other hand, the results reported here lead to the proposal of Phe255, Phe24, and Tyr169 as key residues because they have strong van-der-Waals contacts with the ligand. Furthermore, many of the residues involved in ligand binding are conserved between these three enzymes (1AQU, 1CJM, and bSULT1A1) [12, 25]. For example, in these three enzymes, His108 forms a hydrogen bond with ligand. To the best of our knowledge, Phe24, Phe142, and Tyr169 are conserved in these three enzymes and may be important for structural integrity or maintaining the hydrophobicity of the ligand-binding pocket. In addition, as well as the others in Tables 2 and 3, these residues are suggested as candidates for further experimental studies of structure–function relationships.

Acknowledgements This work was supported by the National Science Foundation of China (20333050, 20073014), Doctor Foundation by the Ministry of Education, Foundation for University Key Teacher by the Ministry of Education, Key subject of Science and Technology by the Ministry of Education of China, and Key subject of Science and Technology by Jilin Province.

References

1. Roy AB (1981) Sulfation of drugs and related compounds. In: Mulder GJ (ed) CRC Press, Boca Raton, FL, pp 83–130
2. Matsui M, Homma H (1994) Int J Biochem 26:1237–1247
3. Falany CN, Wilborn TW (1994) Adv Pharmacol 27:301–329
4. Raftogianis RB, Wood C, Otterness DM, van Loon JA, Weinshilboum RM (1997) Biochem Biophys Res Commun 239:298–304
5. Wang Y, Spitz MR, Tsou AM-H, Zhang K, Makan N, Wu X (2002) Lung Cancer 35:137–142
6. Weinshilboum RM, Otterness DM (1994) Sulfotransferase enzymes. In: Kauffman FC (ed) Conjugation–deconjugation reactions in drug metabolism and toxicity. Chapter 22, "Handbook of experimental pharmacology" series, vol 112. Springer-Verlag, Berlin Heidelberg, pp 45–78

7. Falany CN (1991) Trends Pharmacol Sci 12:255–259
8. Leach M, Cameron E, Fite N, Stassinopoulos J, Palmreuter N, Beckmann JD (1999) Biochem Biophys Res Commun 261:815–819
9. Gamage NU, Duggleby RG, Barnett AC, Tresillian M, Latham CF, Liyou NE, McManus ME, Martin JL (2003) J Biol Chem 278:7655–7662
10. Otterness DM, Her C, Aksoy S, Kimura S, Wieben ED, Weinshilboum RM (1995) DNA Cell Biol 14:331–341
11. Her C, Aksoy IA, Kimura S, Brandriff BF, Wasmuth JJ, Weinshilboum RM (1995) Genomics 29:16–23
12. Kakuta Y, Negishi M, Pedersen LC (1997) Nat Struct Biol 4:904–908
13. InsightII, Version 98.0 (1998) Accelrys Inc. San Diego, USA
14. Homology User Guide (1999) Accelrys Inc. San Diego, USA
15. Lipman DJ, Pearson WR (1985) Science 227:1435–1441
16. Pearson WR, Lipman DJ (1988) Proc Natl Acad Sci USA 85:2444–2448
17. Pearson WR (1990) Meth Enzymol 183:63–98
18. Needleman SB, Wunch CD (1970) J Mol Biol 48:443–453
19. Bernstein FC, Koetzle TF, Williams GJB, Meyer EF Jr, Brice MD, Rodgers JR, Kennard O, Shimanouchi T, Tasumi M (1977) J Mol Biol 112:535–542
20. Discover3 User Guide (1999) Accelrys Inc. San Diego, USA
21. Luthy R, Bowie JU, Eisenberg D (1992) Nature 356:83–85
22. Profile-3D User Guide (1999) Accelrys Inc. San Diego, USA
23. Binding Site Analysis User Guide (1999) Accelrys Inc. San Diego, USA
24. Bidwell LM, Mcmanus ME, Gaedigk A, Kakuta Y, Negishi M, Pedersen JL, Martin L (1999) J Mol Biol 293:521–530
25. Li YF, Hata Y, Fujii T, Hisano T, Nishihara M, Kurihara T, Esaki N (1998) J Biol Chem 273:15035–15044
26. Affinity User Guide (1999) Accelrys Inc. San Diego, USA
27. Tulik GR, Chodavarapu S, Edgar R, Giannunzio L, Langland A, Schultz B, Beckmann JD (2002) J Biol Chem 277:39296–39303